Egypt. J. Chem. **Vol. 65,** No. SI:13B pp. 339-346 (2022)

Egyptian Journal of Chemistry

http://ejchem.journals.ekb.eg/

Hydroxyapatite/ Chitosan Coating By Electrophoretic Deposition on SS 316L For Biomedical Application

Israa Zuhair Ahmed ,[a] Hussein Alaa Jaber ,[b] Shayma M. Salih [a,b,*]

[a] *MSc. Student, Material Engineering Department, University of Technology, Baghdad, ,Iraq-.*

[b] *Asst. Prof. Dr. Material Engineering Department, University of Technology, Baghdad, Iraq*

[c] *Lec. Dr, Material Engineering Department, University of Technology, Baghdad, Iraq*

Abstract

Despite significant and effective progress in metallic orthopaedic applications and bone replacement, there are still challenges and issues. The performance of composite materials in biological devices is heavily influenced by coating processes. Coating composite materials for biomedical purposes is a critical step in increasing their characteristics. Bio coating layers were prepared by pulsed EPD 316L SS substrate using Nano hydroxyapatite powder in chitosan. Hydroxyapatite-chitosan (HAP-CS) was coated on 316L stainless steel utilizing a pulsed electrophoretic deposition (PEPD) process at a constant voltage (30 V) and frequency (50 Hz). X-ray diffraction spectroscopy (XRD), micro roughness testing, and scanning electron microscopy (SEM) were used to examine the deposited coatings, and the Zeta potential for suspensions was computed. The characterisation of the chitosan – hydroxyapatite coating on 316L stainless steel was investigated in this work.

Keyword: Biomedical , pulsed, EPD

1.Introduction

The demand for bone replacement has grown in both young and, old individuals in recent years. Damaged tissues in the human body have the ability to self - reconstruct after any harm. When a damaged tissue or bone is too large to repair, the bone as well as the function of surrounding tissues, are lost. In such case, innovative, alternative materials for bone reconstruction may be utilized [1,2]. Electrophoretic deposition (EPD) is flexible method for treating colloidal suspensions of particulate materials. It has been applied to a wide range of applications, including thin film manufacturing, multi-layered composites, mechanically graded materials, hybrid materials, and micro- patterned colloidal assemblies. The application of pulsed DC as a generic method to monitor bubble integration and obtain bubble- free deposits during aqueous EPD. The application of Pulsed EFD method to control bubble incorporation and obtain bubble-free deposits during aqueous EPD. Hydroxyapatite (HAP) has been employed as a coveringfor metallic body implants because of its biocompatibility, bioactivity, and closeness to the chemical structure of the inorganic component of bone tissue. One of the most promising technologies for generating coatings is electrophoretic deposition. This method is very easy and adaptable, and it may be used to coat any complex formed product in a consistent manner. Chitosan has a wide range of uses in biomedical research, it has also been employed as a coating material for surface change of orthopaedic implants because of its physicochemical features and similarity to the extracellular matrix of bone and cartilage. Biocompatibility, non-toxicity, biodegradability, antibacterial activity, and chemical tolerance are just a few of the qualities[3,4]. To begin with, it consists of suspension-related parameters. EPD- specific parameters including coating time, duty duration, and hydroxyapatite concentration at a constant applied voltage (30V) and frequency (50Hz). The aim of this research is to study the effect coating of HAP/CS on the 316L SS by PEFD to improve biocompatibility of the surface[5,6].

2.Experimental materials and methods

2.1 Materials used

The 316L SS alloys are used as the study substrate, hydroxyapatite (HAP) that Nano powder with the formula Ca5(OH)(PO4)3 (primary particle size of 40 nm) was utilized to deposit a coating layer on 316L SS and purity (96%), melting temperature 1100 C, and molecular weight 502.31g/mol. Chitosan (CS) was used as a binder with HAP powder, having the formula (C8H13O5N) n. The suspension

*Corresponding author e-mail: I3o22oo@uotechnology.edu.iq.; (Shayma M. Salih).

Receive Date: 11 March 2022, Revise Date: 30 April 2022, Accept Date: 17 May 2022

DOI: 10.21608/EJCHEM.2022.126733.5624

preparation was ethanol absolute (purity 99.9%), the formula (C2H5OH). In this research, acetic acid with the formula CH3COOH with and purity 99.7%.

.

2.2 Preparation of substrate

The processes are utilized to make 316L SS samples with a uniform surface that are 1.5 cm * 1.5 cm * 0.1 cm in size. Flat specimens are used as final specimens. To polish sample surfaces to a consistent finish, more silicon sheets (400, 500, and 600 grit) are needed than carbide (SiC) sheets. To eliminate pollutants, polished surfaces are washed with water, cleaned with methanol, rinsed with deionized water, and finally dried with air [7].

2.3 Preparation of suspension

The preparation of aqueous suspensions is an important step in the pulsed electrophoretic deposition (PEPD) experiment. In a 100 mL glass beaker, dissolve 0.05g/100 mL of CS in 1 mL of acetic acid .After that, the glass beaker was filled with a mixture of 79% ethanol and 20% deionized water. After 15 minutes of magnetic stirring , Nano powders of various concentrations ranging from 0.15g/100 mL to 0.6g/100 mL HAP) were added, the four Nano hydroxyapatite suspensions used in the study are shown in figure (3.2).

Finally, to break up weak agglomerates and disperse the particles in the suspension, sonication in an ultrasonic bath (for 20 min) is utilized [4,5]. The pH meter with acetic acid was used to modify the pH range of the suspensions at (4.5- 5).

2.4 EPD technique

In pulsed electrophoretic deposition 316L SS was used as counter electrodes (anode) and working electrodes (cathode). Before deposition the cathode and anodic electrodes were washed in ethanol and dried, which a success by immersing them in a 100 ml beaker filled with solution. The electrode spacing was kept stable at 10 mm in the EPD cell and only 1.8 cm^2 of substrate was exposed to deposition.

The deposited samples were deleted from the bath after the deposition operation and dried overnight in an air surroundings by varying the deposition period (from 10 to 20 min) and providing constant voltage. The system of pulsed EPD was explained in the figure 1.

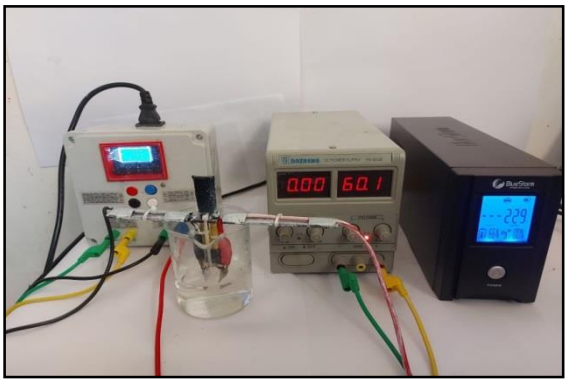

Fig.1. The system of pulsed EPD

3. Specimens Grouping

The specimens that were coated with various compositions of HAP/CS coat materials. In this part was clarified the coating specimen groups for HAP/CS coat materials of varied compositions on 316L SS as a substrate.

Table 1: .Coating specimen groups for HAP/CS coat materials of numerous compositions on the 316L SS at 30 V

	Group A 316L SS (Frequency=50 Hz)					Group B 316L SS (Frequency=300 Hz)			
	Samples	Conc. HAP g/100mL	Time of Dep. T(min)	% Duty		Samples	Conc. HAP g/100mL .	Time of Dep. T(min)	% Duty
A1	S1	0.15	10	25	B1	S37	0 .15	10	25
	S2	0.30	10	25		S38	0.3	10	25
	S3	0.45	10	25		S39	0.45	10	25
	S4	0.6	10	25		S40	0.6	10	25
	S5	0 .15	10	50		S41	0 .15	10	50
	S6	0 .3	10	50		S42	0.3	10	50
	S7	0 .45	10	50		S43	0.45	10	50
	S8	0 .6	10	50		S44	0.6	10	50
	S9	0.15	10	75		S45	0.15	10	75
	S10	0 .3	10	75		S46	0.3	10	75
	S11	0 .45	10	75		S47	0.45	10	75
	S12	0 .6	10	75		S48	0.6	10	75
A2	S13	0 .15	15	25	B2	S49	0.15	15	25
	S14	0 .3	15	25		S50	0.3	15	25
	S15	0 .45	15	25		S51	0.45	15	25
	S16	0 .6	15	25		S52	0.6	15	25
	S17	0.15	15	50		S53	0.15	15	50
	S18	0 .3	15	50		S54	0.3	15	50

	S19	0 .45	15	50		S55	0.45	15	50
	S20	0 .6	15	50		S56	0.6	15	50
	S21	0 .15	15	75		S57	0.15	15	75
	S22	0.3	15	75		S58	0.3	15	75
	S23	0 .45	15	75		S59	0.45	15	75
	S24	0 .6	15	75		S60	0.6	15	75
	S25	0.15	20	25		S61	0.15	20	25
	S26	0.3	20	25		S62	0.3	20	25
	S27	0.45	20	25		S63	0.45	20	25
	S28	0.6	20	25		S64	0.6	20	25
	S29	0.15	20	50		S65	0.15	20	50
	S30	0.3	20	50		S66	0.3	20	50
	S31	0.45	20	50		S67	0.45	20	50
A3	S32	0.6	20	50	B3	S68	0.6	20	50
	S33	0.15	20	75		S69	0.15	20	75
	S34	0 .3	20	75		S70	0.3	20	75
	S35	0 .45	20	75		S71	0.45	20	75
	S36	0 .6	20	75		S72	0.6	20	75

4.Characterization of samples

4.1 Zeta potential The stability of the suspensions and the homogeneity of the coatings were inspected by zeta potential.

This experiment was carried out at Baghdad University of Technology's Nanotechnology and Advanced Materials Research Centre. Model: Zeta Plus Signal Processing: Electrophoretic Light Scattering, ELS Precision: ± 3%, depending on salt concentration Standard Laser: 35 mW red diode laser, nominal 640 nm wavelength. The four suspension concentrations were employed (0.15,0.3,0.45,0.6) g/100 mL[8,9].

4.2 X-ray diffraction (XRD)

X-ray diffraction apparatus (XRD) (XRD-6000, NF type) with Cu target (K1 of 1.54060) Model: X R D-6000 X- Ray Tube: Cu, NF type) with Cu target, X-Ray leakage is less than 2.5Sv/h. The peaks were then compared to the standards peaks for each substance using JCPDS cards (joint committee on powder diffraction standards). Scherer formula was used to determine the crystallite size (particle size) of the HAP powder and HAP/CS composite coating [10,11].

4.3 Scanning Electron Microscopy and Energy Dispersive X-Ray Spectroscopy (EDX).

Field Emission Scanning Electron Microscopes (FESEM) are scientific devices that utilize a high-energy electron beam to analyze things at a very fine scale and image features as tiny as 10 nm. Scanning electron microscopy (SEM) combines high-resolution imaging with element analysis, making it a useful tool. This inspection may provide information regarding topography (characterizing an object's surface properties and identifying the natural of the fracture process) morphology and the fracture process (the form and size of the object's particles).The distribution of elements in the coatings layer was also detected using an Energy Dispersive X-ray Spectrometry (EDX) detector. EDX was utilized to determine the atomic proportion of elements. This test was carried out in the Islamic Republic of Iran using Mira3 TESCAN equipment.

4.4 Vickers micro hardness Test

The micro hardness test consider as one of the important mechanical testing for materials. The surface hardness of the composite coating was checked at the University of Technology's Materials Engineering Department using (Time Group INC Beijing) equipment by applying a load (9.8N) and holding it for 45 % for coated samples. Three values were recorded for the amount of indentation that was putted amorphous a square based pyramid diamond indenter. The Vickers micro hardness test was used to calculate out the hardness of 316L SS substrates. Micro hardness tester by Vickers (Digital Micro Vickers Hardness Tester model TH-714).

5.Characterization of the basic materials and coated samples

5.1 Zeta potential

Zeta potential measurements were performed to better understand the suspension stability and deposition process. At different hydroxyapatite concentrations (0.3, 0.45, and 0.6) g/100 mL HAP, the zeta potentials of suspensions containing HAP/CS were (9.39, 27.13, and 18.74) mV, respectively. Suspension zeta potential values were found to be positive. This shows that the HAP nanoparticles are deposited than cathode, yet the HAP/CS composite has a negative value (0.15g/ 100 mL)-13.43 mV. Furthermore, suspensions containing (0.3, 0.45, and 0.6) g/100 mL HAP had high mobility values of (0.18, 2.08, and 0.37) m^2/s. V.

while suspensions containing 0.15g/100 mL had mobility value of (-0.26 m2/s. V), it was discovered

that using the hydroxyapatite concentration (0.45 g/100 mL), the zeta potential and value mobility are maximum (27.13 mV and 2.08 cm^2/V.s, respectively), resulting in a very stable suspension that would boost the deposition rate throughout the EPD process.

The generated (H+) ions may absorb on the surface of CS and HAP nanoparticles, increasing the positive surface charge and, as a consequence, the zeta potential of the HAP/CS particles.

As a result, charged colloidal particles in suspension would have superior electrostatic stability, with a higher electrostatic charge on the particles resulting in a faster deposition rate.

Furthermore, raising the concentration of hydroxyapatite (0.15g/100 mL) increased the ionic strength of the suspension and reduced the thickness of the double layer, reducing the particles zeta potential and decreasing suspension stability. In addition, this solution had a pH of 4.5.

The pH of the suspension may be adjusted to control particle agglomeration and suspension stability. A pH of (3.5 - 4.5) has been shown to enhance particle surface electrostatic charge and deposition rate, resulting in a higher deposit density[12-15].

5.2 XRD of hydroxyapatite powder

The XRD patterns for HAP powder at (002) (211), (300), (310), and (213) were the values for the HAP peaks determined to be at 25.9289°, 32.0837°, 33.0398°, 40°, and 49°.

It had been given to (JCPDS 09-0432) for pure HAP. The reduction in crystallite size is primarily responsible for the widening of XRD peaks, demonstrating the powder's the Nano crystal line nature. In the neutral state, stoichiometric HAP is stable.

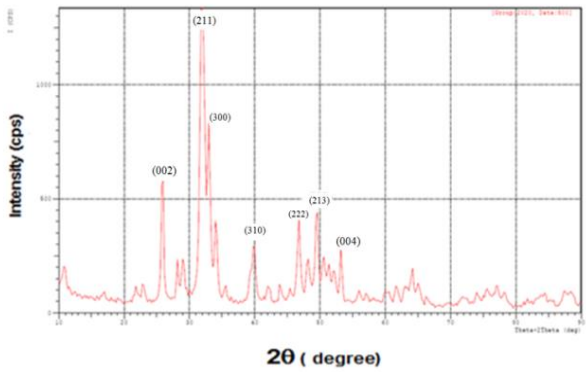

Fig. 2.The XRD pattern of HAP

All of the diffraction lines for stoichiometric HAP were compatible with JCPDS file No. 9-432. The average crystallite size of regular HAP powder is approximately 16.8 nm, as indicated in table (2). As it can be seen from the above table (4.3) that the average crystallite size is about 16.8 nm, which is demonstrates the approximate particle size of the used HAP.

Table 2:The top three the Nano HAP peaks have different crystallite sizes.

Peak	2θ	Cos θ	FWHM (degree)	λ (A^O)	D = 0.9λ / FWHM Cos θ (nm)
1	32.08	0.961	1.091	1.5406	13.2
2	33.03	0.958	0.773	1.5406	18.7
3	25.92	0.974	0.762	1.5406	18.6
D average = 16.8 nm					

Using the analytical methodology outlined in reference, lattice parameters crystalline planes standard HAP were obtained. All diffraction peaks identical with (JCPDS card the No 09-432) peaks standard HAP, the diffraction pattern of HAP powder explain in the figure (2).

5.3 XRD of substrate material (316L SS)

The XRD method was utilized to identify phases in S316L SS, including Nano hydroxyapatite and HAP coated, prior to coating. JCPDS file numbers 33-0397 match the austenite diffraction lines. In the diffraction planes (111), (200), and (300), austenite peaks may be detected (220). Table 4.4 demonstrates that the average crystallite size of S316L SS is around 25 nm; table 3 explains the crystallite size of the top three S316L SS peaks; and picture 3 depicts the XRD of the as received 316L SS.

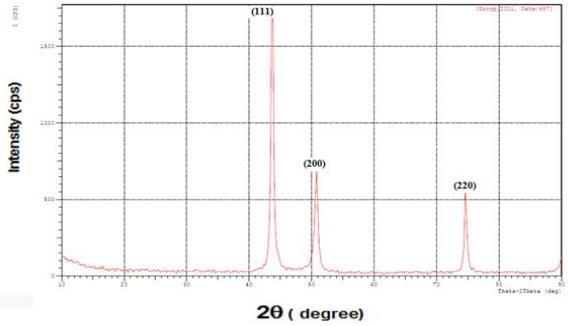

Fig. 3.XRD of as received 316L SS.

Table 3: Crystallite size highest three peeks S316L SS.

sample	2θ	FWHM (degree)	Crystal size(D) nm D = 0.9 λ/ FWHM Cosθ	Average crystal size (nm)
S316L	43.7107	0.630	23.7	25.07
	50.73	0.731	21	
	74.62	0.572	30.5	

5.4 XRD Characterization of HAP/CS coating layer by Pulsed EPD

Table 4 depicts the X-ray diffraction patterns of a composite deposit for samples S30, S31, and S32 in group A3 as a function of hydroxyapatite content. At a frequency of 50 Hz, a deposition duration of 20 minutes, and a duty cycle of 50%, the S316L SS was coated with different concentrations of hydroxyapatite (0.30, 0.45, and 0.60) g/100 mL. The XRD study of the coating reveals a high degree of crystalline with no change in crystal structure. Furthermore, because there is no contact between the coating particles. Figure 4 was showed XRD of samples S30, S31and S32 as different of concentration HAP(0.30,0.45 and 0.6) g/100 mL respectively, time of deposition 20 min, duty cycle 50%, at frequency 50 Hz [16-18].

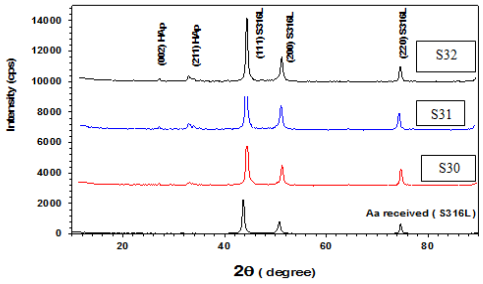

Fig.4 The XRD of samples S30, S31 and S32 as different of concentration HAP (0.30, 0.45 and 0.6) g/100 mL respectively ,time of deposition 20 min, duty cycle 50%, at frequency 50 Hz.

Table 4:XRD diffraction peaks and crystal size calculation of S316L SS and time of deposition 20 min, at frequency 50 Hz.

Sample	2theta degree	FWHM (degree)	I	Crystal size(D) nm D = 0.9 λ/ βCosθ	Average crystal size (nm)
S316L peaks					
S30	43.82	0.600	100	24.8	25.7
	50.83	0.643	37	23.8	
	74.70	0.609	29	28.6	
S31	43.77	0.615	100	24.2	24.7
	50.79	0.712	36	21.5	
	74.67	0.612	24	28.4	
S32	43.72	0.648	100	23	24.2
	50.733	0.719	38	21.3	
	74.65	0.610	26	28.5	
HAP peaks					
S30	32.30	1.066	5	13.5	13
S31	32.22	0.9600	8	15	18.7
	33.23	0.6400	5	22.5	
S32	32.20	0.979	9	14.7	20.8
	33.03	0.673	5	21.4	
	26.05	0.539	4	26.3	

5.5 Micro roughness characterization of HAP/CS coating layers on S316 L SS by EPD

The micro roughness of the HAP/CS coating layer generated on S316L SS as a function of HAP concentration values is shown in Figure 5 (a, b). Figure 5 (a) shows that when HAP concentrations increase, the micro roughness of the HAP/CS coated layer increases due to porosity and large grain formation. However, a higher micro roughness value is obtained at deposition pulse frequency (50) Hz than at pulse frequency (300) Hz, which is associated to the creation of a considerable porosity density. Furthermore, with increasing HAP concentrations at 50 Hz and extended deposition time, figure 5 (b) shows random increases and decreases in the micro roughness of the HAP/CS coated layer. This demonstrates that as coating thickness grows, the porosity of the coating increases, resulting in a uniform distribution of HAP as well as a thick coating layer that seems to be broken due to the high HAP/CS particle concentration.

Fig. 5. Micro roughness of HAP/CS coating layer (a) T= 10 min, (b) T= 15 min

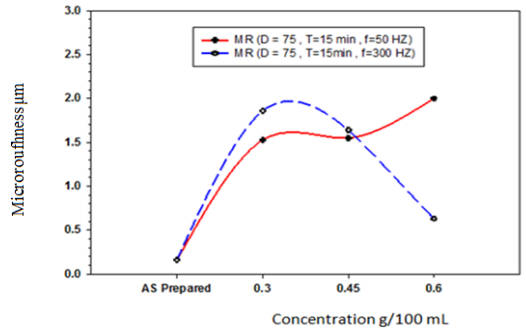

(b)

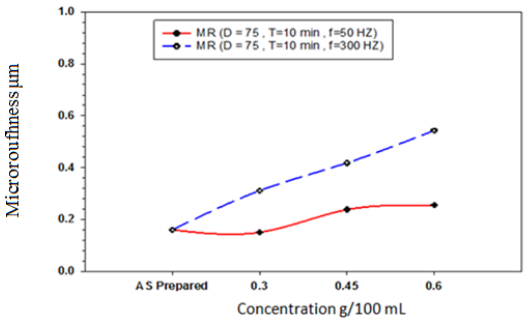

(a)

5.6 Field emission scanning electron microscopy (FE-SEM) and energy dispersive X-Ray spectroscopy (EDX) of HAP/CS coating layers on S316 L SS by pulsed EPD.

In group (B) studies, figures 6 and 7, FE-SEM pictures of 0.6 g/100 mL HAP/composite coatings layers placed on the S316L SS substrate at varying deposition durations (10, 15, and 20) min with a pulse frequency of 300 HZ and a duty cycle of 75% are presented (a, b, and c). Sample S48's microstructure was not well packed, resulting in an aggregation of nonhomogeneous particle distribution seen in the coating. Because of the high pulse frequency and extended deposition duration, it creates a high porosity structure as well as coating breakdown, resulting in nonhomogeneous coatings. This result is shown in the diagram (6.a). At F 300 Hz, Figure 6.b shows a broken aggregate structure with a nonhomogeneous particle distribution. The use of high frequency values throughout the EPD process resulted in a considerable increase in coating porosity and a greater likelihood of fracture formation. Furthermore, coarse particles will be deposited, increasing the coating's roughness and increasing the likelihood of breaking in the thick layer. In the figure (6.c) for the sample S72.Finally, if the EPD frequency is high, the nanoparticles travel quickly toward the charge electrode on the other side, where they not have enough time to settle into a suitable position to produce a homogeneous coating [19-24].

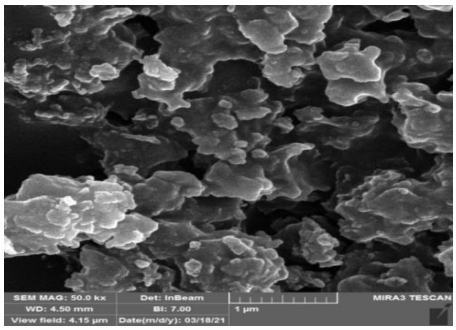

(a)

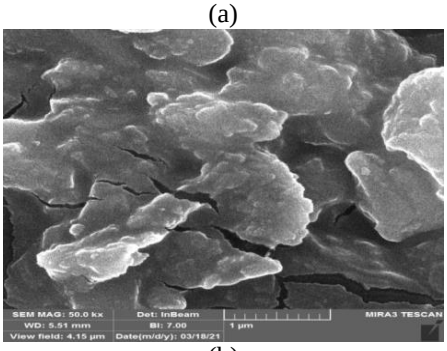

(b)

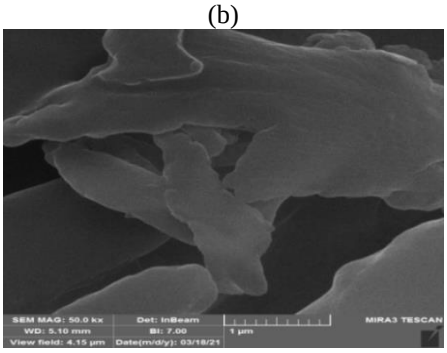

(c)

Fig. 6. FE-SEM images of 0.6g/100 mL HAP/CS on S316L deposited at different time (a) 10min for S48, (b) 15 min for S60 and (c) 20 min for S72, at constant (F 300 Hz, D =75%).

6. Conclusion

On 316LSS substrates, the pulsed electrophoretic deposition method was effectively used to produce a HAP/CS coat. The higher zeta potential value of 27.13 mV with mobility of 2.08 $cm^2/V.s$ for concentration of hydroxyapatite 0.45g/100mL. The XRD for the substrate 316L SS and hydroxyapatite powder was measured in this study to obtain the diffraction pattern.

7. Conflicts of interest

The authors declare that they have no conflict of interest.

8. Acknowledgments

I would like to express my deep thanks to the staff of Material Engineering Department, University of Technology and staff Nano Technology Centre, (University of Technology.) to characterization of the coated samples.

9. References

[1] X. Zhao, L. Zhang, X. Wang, J. Yang, F. He and Y. Wang, Preparation and mechanical properties of controllable orthogonal arrangement of carbon fiber reinforced hydroxyapatite composites, *Ceramics International*, Vol. 44, No. 7, PP. 8322- 8333, (2018).

[2] R. Aminatun , D. Hikmawati , P. Widiyanti , T. Amrillah , A. Nia, I. Firdania, C. Abdullah, Study of mechanical and thermal properties in nano hydroxyapatite/ chitosan/ carbon-methyl cellulose nano composite-based scaffold for bone tissue engineering the roles of carbon- methyl cellulose, *Applied Since*, Vol. 7, No.8, pp.23, (2020), https://doi.org/10.3390/app10196970.

[3] Jasim, M., Abbass, M. K., Salah, K., & Jasim, A. N. (2020, March). Characterization of electrophoretic deposition parameters of nano hydroxyapatite coating on the Ti6Al4V alloy using DC current. In *AIP Conference Proceedings* (Vol. 2213, No. 1, p. 020203). AIP Publishing LLC.

[4] T. Matsushita, H. Takahashi, Orthopaedic applications of metallic biomaterials, metals for biomedical devices. *Elsevier Ltd. All rights reserved*, Vol. 2068, No. 2, PP. 149- 154, (2019). https://doi.org/10.1016/B978-0-08-102666-3.00017-1.

[5] A. Molaei, M. Yousefpour, Electrophoretic deposition of chitosan bioglass- hydroxyapatite–halloysite nanotube composite coating, *RARE METALS*, https://doi.org/10.1007/s12598-018-1021-2, (2018).

[6] Bartmanski, M., Zielinski, A., Jazdzewska, M., Głodowska, J., & Kalka, P. (2019). Effects of electrophoretic deposition times and nanotubular oxide surfaces on properties of the nanohydroxyapatite/nanocopper coating on the Ti13Zr13Nb alloy. *Ceramics International*, *45*(16), 20002-20010.

[7] Singh, S., Singh, G., & Bala, N. (2020). Electrophoretic deposition of hydroxyapatite-iron oxide-chitosan composite coatings on Ti–13Nb–13Zr alloy for biomedical applications. *Thin Solid Films*, *697*, 137801.

[8] Fajri, H., Ramadhan, F., Nuswantoro, N. F., Juliadmi, D., Tjong, D. H., Manjas, M., ... & Yetri, Y. (2020). Electrophoretic deposition (EPD) of natural hydroxyapatite coatings on titanium Ti-29Nb-13Ta-4.6 Zr substrates for implant material. In *Materials Science Forum* (Vol. 1000, pp. 123-131). Trans Tech Publications Ltd.

[9] Oliveira, J. A. M., de Santana, R. A. C., & Neto, A. D. O. W. (2020). Characterization of the chitosan-tungsten composite coating obtained by electrophoretic deposition. *Progress in Organic Coatings*, *143*, 105631.

[10] Ahmed, Y., & Rehman, M. A. U. (2020). Improvement in the surface properties of stainless steel via zein/hydroxyapatite composite coatings for biomedical applications. *Surfaces and Interfaces*, *20*, 100589.

[11] Akram, M., Arshad, N., Aktan, M. K., & Braem, A. (2020). Alternating Current Electrophoretic Deposition of Chitosan–Gelatin–Bioactive Glass on Mg–Si–Sr Alloy for Corrosion Protection. *ACS Applied Bio Materials*, *3*(10), 7052-7060.

[12] Sivaraj, D., & Vijayalakshmi, K. (2019). Enhanced antibacterial and corrosion resistance properties of Ag substituted hydroxyapatite/functionalized multiwall carbon nanotube nanocomposite coating on 316L stainless steel for biomedical application. *Ultrasonics sonochemistry*, *59*, 104730.

[13] Ruqaya M. Hamid Al-Sultan, Ammar Abdulsalaam Al-Sultan, Mohammed A. Hayawi, Bilal J M Aldahham, Mohanad Y. Saleh, Hazim A. Mohammed. The effect of subclinical thyroid dysfunction on B- type natriuretic peptide level. Revis Bionatura 2022;7(2) 21. http://dx.doi.org/10.21931/RB/2022.07.02.21

[14] Saeed, N. H. M., & Abbas, A. M. (2020). Kinetics and mechanism of tetrahydrofuran oxidation by chloraminet in acidic media. Periodico Tche Quimica, 2020, 17(35), pp. 449–461.

[15] Pokhrel, S. (2018). Hydroxyapatite: preparation, properties and its biomedical applications. *Advances in Chemical Engineering and Science*, *8*(04), 225.

[16] George, S., Mehta, D., & Saharan, V. K. (2020). Application of hydroxyapatite and its modified forms as adsorbents for water defluoridation: an insight into process synthesis. *Reviews in Chemical Engineering*, *36*(3), 369-400.

[17] Pawlik, A., Rehman, M. A. U., Nawaz, Q., Bastan, F. E., Sulka, G. D., & Boccaccini, A. R. (2019). Fabrication and characterization of electrophoretically deposited chitosan-hydroxyapatite composite coatings on anodic titanium dioxide layers. *Electrochimica Acta*, *307*, 465-473.

[18] Mahmoud Shaker Nasser, Electrophoretic Deposition of Hydroxyapatite / Titanium Oxide Nano-composite Coatings on Duplex Stainless Steel for Biomedical Applications, submitted to of Faculty Engineering University of Kufa *By* Prof. Dr. Ali Sabea Hammond, (2020).

[19] R. Pillai, M. F. and V. Sglavo, HA/ β- TCP plasma sprayed coatings on Ti Substrate for Biomedical Application, Ceramics International, Vol. 44, No. 2, PP. 1329-1333, (2018).

[20] Aldahham, B. J., Al-Khafaji, K., Saleh, M. Y., Abdelhakem, A. M., Alanazi, A. M., & Islam, M. A. (2020). Identification of naphthyridine and quinoline derivatives as potential Nsp16-Nsp10 inhibitors: a pharmacoinformatics study. Journal of Biomolecular Structure and Dynamics, 1-8.

[21] Abdullah, J. A., Yhya, R. K., & AL-Sayd Toohi, H. T. (2021). Synthesis of some Imidazolidinone compounds under phase transfer conditions and photo cleavages studies of molecular for these compounds. Egyptian Journal of Chemistry, 64(12), 2-3.

[22] Ayoob, A., Sadeek, G., Saleh, M. (2022). Synthesis and Biologically Activity of Novel 2-Chloro -3-Formyl -1,5-Naphthyridine Chalcone Derivatives. *Journal of Chemical Health Risks*, 12(1), 73-79. doi: 10.22034/jchr.2022.688560

[23] Al-Thakafy, N., Al-Enizzi, M., Saleh, M. (2022). Synthesis of new Organic reagent by Vilsmeier – Haack reaction and estimation of pharmaceutical compounds (Mesalazine) containing aromatic amine groups. *Egyptian Journal of Chemistry*, 65(6), 685-697. doi: 10.21608/ejchem.2021.101851.4729

[24] Toohi, H. T. A. S., Rabeea, M. A., Abdullah, J. A., & Muslim, R. F. (2021). Synthesis and characterization activated carbon using a mix (asphalt-polypropylene waste) for novel azo dye (HNDA) adsorption. Carbon Letters, 31(5), 837-849.